Check for updates

Proceedings of the ASME 2020
Verification and Validation Symposium
VVS2020
May 20-22, 2020, Virtual, Online

VVS2020-8816

Downloaded from http://asmedigitalcollection.asme.org/VVS/proceedings-pdf/VVS2020/83594/V001T03A002/6554370/v001t03a002-vvs2020-8816.pdf by Clemson University user on 09 February 2022

IMPROVING THE INTERPRETABILITY OF PHYSICS-BASED BIAS IN MATERIAL MODELS

Evan Chodora*
Department of Mechanical Engineering
Clemson University
Clemson, South Carolina 29634

Garrison Flynn
E-2: Process Modeling and Analysis
Los Alamos National Laboratory
Los Alamos, New Mexico 87545

Trevor Tippetts & Cetin Unal
E-13: Advanced Engineering Analysis
Los Alamos National Laboratory
Los Alamos, New Mexico 87545

ABSTRACT

In order to accurately predict the performance of materials under dynamic loading conditions, models have been developed that describe the rate-dependent material behavior and irrecoverable plastic deformation that occurs at elevated strains and applied loads. Most of these models have roots in empirical fits to data and, thus, require the addition of specific parameters that reflect the properties and response of specific materials. In this work, we present a systematic approach to the problem of calibrating a Johnson-Cook plasticity model for 304L stainless steel using experimental testing in which the parameters are treated as dependent on the state of the material and uncovered using experimental data. The results obtained indicate that the proposed approach can make the presence of a discrepancy term in calibration unnecessary and, at the same time, improve the prediction accuracy of the model into new input domains and provide improved understanding of model bias compared to calibration with stationary parameter values.

INTRODUCTION

In order to accurately predict the performance of materials under dynamic loading conditions, such as those encountered in metal forming operations, high speed impacts, or explosive deformations, much work has been carried out to try and describe the complex, strain rate-dependent material behavior and irrecoverable plastic deformation that occurs at elevated strains and applied loads [1]. A wide number of computational models have been developed to describe this viscoplastic phenomenon, such as the Mechanical Threshold Stress (MTS) model [2, 3], the Zerilli-Armstrong model [4], and the Preston-Tonks-Wallace (PTW) model [5]. These various methods try to improve the ability of scientists and engineers to predict material behavior by incorporating various dislocation mechanics, hardening physics, and thermodynamic effects that are present in materials under loading. Other models that are commonly used include the Johnson-Cook [6] and the Steinberg-Cochran-Guinan-Lund (SCGL) [7, 8] flow stress models.

Most of these models have roots in empirical fits to data, which can lead to difficulty in extrapolating to new material systems. Thus, these models require the addition of specific parameters that reflect the properties and response of new materials. The appropriate values of these parameters may not be exactly known, however, so the application of techniques in the field of model calibration becomes an important resource to both achieve model accuracy and quantify output uncertainty. Accuracy, as well as interpretability, of model calibration becomes especially important in cases where experimental testing may not be available in the input domain of the true system and the model is, therefore, forced to extrapolate when used as a predictor.

Model calibration techniques commonly formulate the problem as an attempt to find the set of stationary parameter value distributions that allow the best model fit, on average, to the experimental observations across the input domain. In reality, how-

*Corresponding author: echodor@clemson.edu.

The United States Government retains, and by accepting the article for publication, the publisher acknowledges that the United States Government retains, a non-exclusive, paid-up, irrevocable, worldwide license to publish or reproduce the published form of this work, or allow others to do so, for United States Government purposes.

This material is declared a work of the U.S. Government and is not subject to copyright protection in the United States.
Approved for public release. Distribution is unlimited.

ever, the best values of the calibration parameters often shift according to the model inputs due to an inadequate inclusion of all the true system physics in the underlying model form. Therefore, an additive bias or discrepancy term is often included to account for output inaccuracy across input values. Alternatively, a model calibration approach capable of treating parameter values as functions of the model input can reveal a more interpretable result than discrepancy methods. A better understanding of the input domain to calibration parameter relationships serves to both reduce model output uncertainty and parameter value uncertainty while simultaneously providing valuable information about the physics-based bias present in the model without resorting to using discrepancy terms. The implementation of input state-dependent parameters into the model has the potential to not only improve model accuracy in reproducing experimental observations, but—more importantly—allow for more accurate predictions into untested input domains by better representing missing physics phenomena in the model.

The paper presents a review of several Bayesian model calibration techniques and methods commonly used to tune computer model parameters using experimental data. This review is followed by a presentation of a systematic approach to the problem of calibrating a Johnson-Cook plasticity model for 304L stainless steel using both quasi-static and Hopkinson bar experimental testing in which the parameters are treated as dependent on the input states of the material temperature, strain, and strain rate. The parameter relationship form is established using nonparametric techniques that allow the most likely relationships to be uncovered using the experimental observations without needing to specify a functional form. This procedure is compared to the other Bayesian model calibration formulations with and without both functional parameters and discrepancy. Additionally, the results of the calibrated functional relationships are examined to provide an experimentally-informed and interpretable assessment of the Johnson-Cook model form bias that exists over the input domain. This better understanding of the physics-based bias serves as a direct method to extend the model formulation to improve the model fit for new materials and input domains.

JOHNSON-COOK PLASTICITY MODEL

Johnson-Cook is a purely empirical model that describes the material flow stress according to the following equation [6]:

$$\sigma_y(\varepsilon_p, \dot{\varepsilon}_p, T) = [A + B(\varepsilon_p)^n]\left[1 + Cln\left(\dot{\varepsilon}_p^*\right)\right][1 - (T^*)^m] \quad (1)$$

where ε_p is the plastic strain, $\dot{\varepsilon}_p$ is plastic strain rate, and A, B, C, n, m are constants of the specific material. The normalized plastic strain rate and temperature are computed as:

$$\dot{\varepsilon}_p^* = \frac{\dot{\varepsilon}_p}{\dot{\varepsilon}_{p_0}} \quad (2)$$

$$T^* = \frac{T - T_0}{T_m - T_0} \quad (3)$$

where $\dot{\varepsilon}_{p_0}$ is the quasi-static strain rate of $1.0s^{-1}$ is used to normalize the plastic strain rate, T_0 is a reference temperature (generally room temperature), and T_m is the melt temperature of the material.

The general approach to calibrate the 5 material specific parameters of the model is to collect stress-strain data at both quasi-static strain rates (through traditional tensile testing) and high strain rates (generally through Hopkinson bar tests) across a range of material temperatures [9]. This data can then be used to fit a complement of parameters that best describe the behavior of the material across those strain rates and temperatures. A difficulty arises, however, when it is desired to use the calibrated model at temperatures or strain rates above that which is possible to be tested and measured in a laboratory setting. The Split-Hopkinson Pressure Bar (SHPB) test, for example, is generally limited to strain rates on the order of $10^3 s^{-1}$ with some advanced systems achieving approximately $10^4 s^{-1}$, while the strain rates encountered in Taylor rod impacts (a commonly used test to validate plasticity models) can easily exceed $10^5 s^{-1}$ and can often be even higher [10,11]. Therefore, it becomes important to both understand the uncertainty and be able to validate these calibrated models in regimes of interest, even if they may be outside of experimental data bounds.

Experimental Data

Specifically, the Johnson-Cook model is chosen to be used to calibrate stress-strain experimental data for 304L stainless steel. The data has been collected by the MST-8 group at Los Alamos National Laboratory and the data sets consist of quasi-static, uniaxial tensile testing data and higher strain rate SHPB testing data. Tests at both of the two strain rate magnitude regions have been conducted across a range of material temperatures. The available stress-strain data for the 304L stainless steel is shown in Tab. 1 and plotted in Fig. 1.

A subset of this data is selected to use for each of the subsequent calibration approaches to both retain some data as holdout data and ensure that there is a comparable amount of available data for both temperature and strain rate levels.

CALIBRATION METHODOLOGIES DISCUSSION

Many of the physical behaviors studied in engineering and science are complex and efforts to better understand these processes require experiments that are often economically or technically difficult. Therefore, the use of computer models and simulations to study and better understand these systems are commonly used. The utility of models, however, is directly linked to the ability of the simulation to accurate replicate the real-world phenomenon. This accuracy is dependent upon the process of being able to infer model inputs through a combination

Downloaded from http://asmedigitalcollection.asme.org/VVS/proceedings-pdf/VVS2020/83594/V001T03A002/6554370/v001t03a002-vvs2020-8816.pdf by Clemson University user on 09 February 2022

TABLE 1. STAINLESS STEEL (304L) STRESS-STRAIN EXPERIMENTAL DATA

Test Number	Testing Type	Temp (K)	Strain Rate (1/s)
1	Uniaxial	293	0.001
2	Uniaxial	293	0.1
3	SHPB	293	3250
4	SHPB	473	3700
5	Uniaxial	673	0.001
6	SHPB	673	3600
7	SHPB	873	3500

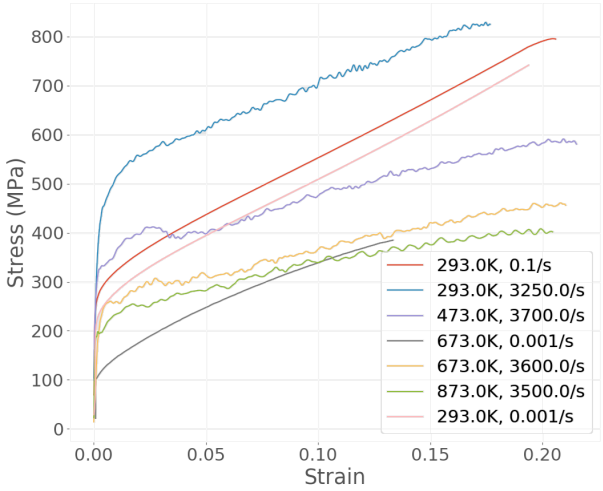

FIGURE 1. PLOT OF THE EXPERIMENTAL STRESS-STRAIN DATA FOR 304L STAINLESS STEEL ACROSS A VARIETY OF TEMPERATURE AND STRAIN RATE SETTINGS

of model predictions and experimental data. This inference process is commonly referred to as model calibration and the popular framework of Bayesian calibration is chosen to analyze in this work. The following four subsections outline the chosen methodologies that will be compared, each of which is a further development of the general Bayesian calibration approach in the following subsections.

Bayesian Calibration

Bayesian model calibration has become a commonly used and widely accepted method for improving computer models using experimental data. The process involves using Bayesian inference to learn about model inputs through the computation of an output likelihood using both the model output and known uncertainties [12, 13]. An advantage of this technique is that it can allow for the incorporation of sources of uncertainty, which can be from a combination of both parameter value uncertainties and experimental error uncertainties. Incorporating uncertainties in this way can provide an additional measure of confidence for the resulting, posterior parameter distributions and also better explain the impact of experimental variation on the parameters values.

Following previous work in the calibration of models with functional output – as is the case with the Johnson-Cook stress-strain curve outputs – the model form and calibration process is followed as in Williams et al. [14] and Bayarri et al. [15] and is

$$y(x) = \eta(x,\theta) + \varepsilon \tag{4}$$

where $y(x)$ is the measured stress values according to the inputs $x = \{\varepsilon_p, \dot{\varepsilon}_p, T\}$, T corresponds to the output of the computer model, η, at the same inputs, θ denotes the vector of unknown model calibration parameters (here representing the five Johnson-Cook model parameters), and ε represents the measurement uncertainty in the experimental data. The calibration process will thus seek to uncover the most likely values for the true, but unknown, values for θ and ε that allow the model to best represent the experimental data. In this approach, the posterior values of θ remain constant throughout the model input domain and will therefore be referred to as "stationary" parameters in this paper.

Letting $\pi(\theta)$ represent the prior distributions of the calibration parameters and $L(\cdot|\cdot)$ represent the likelihood function, the posterior distributions of the parameters takes the form

$$\pi(\theta,\varepsilon|y) \propto L(y|\theta,\varepsilon)\cdot\pi(\theta)\cdot\pi(\varepsilon) \tag{5}$$

that can be effectively explored with the technique of Markov chain Monte Carlo (MCMC). A Gibbs sampler is used to take draws from the distributions [16, 17].

Gaussian Process Discrepancy

It is often the case that even if we were able to know the true values of the model parameters to input to the model, there will be still be some error due to model bias. This model bias, or discrepancy, is thus the difference between the mean output of the true system and the model output at the true parameter values. Following the framework established by Kennedy and O'Hagan [12], we choose to represent this model discrepancy as a Gaussian process (GP) over the model input domain. The posterior distribution of the GP can then serve as a correction term to the model in regions of the domain where there is model bias. Using a GP for this approach has the advantages of both being able to use a nonparametric form for the discrepancy and to apply prior distributions to the GP in the same fashion as the model parameters themselves. The model form used in the calibration procedures thus becomes

$$y(x) = \eta(x,\theta) + \delta(x) + \varepsilon \tag{6}$$

Downloaded from http://asmedigitalcollection.asme.org/VVS/proceedings-pdf/VVS2020/83594/V001T03A002/6554370/v001t03a002-vvs2020-8816.pdf by Clemson University user on 09 February 2022

where $\delta(x)$ represents the additive GP discrepancy term over the same input vector, x, as both the model and experimental data. In this work, the discrepancy is modeled as below using a squared exponential kernel for the covariance function $R(\cdot,\cdot)$ [18]:

$$\delta(x) \sim GP(\mu(x), R(x,x')) \tag{7}$$

$$R(x,x') = \sigma^2 exp\left(\frac{-(x-x')^2}{2l^2}\right) \tag{8}$$

where $\mu(x)$ is the mean function of the GP (treated as mean zero in this case), σ^2 is the variance of the GP kernel, and l is the length-scale of the kernel. The variance and length-scale terms are generally referred to as the "hyperparameters" of Gaussian process and become additional parameters for which to determine the posterior distributions during the model calibration process.

Thus with this GP discrepancy formulation, the Bayesian form of the problem representing the posterior distributions of the parameters in Eqn. 5 becomes

$$\pi(\theta,\varepsilon,\sigma,l|y) \propto L(y|\theta,\varepsilon)\cdot\pi(\theta)\cdot\pi(\varepsilon)\cdot\pi(\sigma)\cdot\pi(l) \tag{9}$$

where now the posterior distributions of the calibration parameters, experimental error, and the GP hyperparameters are explored simultaneously using MCMC.

State-Dependent Parameter Calibration

Similar to the idea that a model may be inadequate in representing the experimental output in one or more regions of the input domain, it is often common that the best posterior values for the calibration parameters may shift according to the subset of the input space considered for calibration [19–21]. In these cases, it would make sense to then treat the parameters themselves as functions of the model inputs. In this approach, we establish each model parameter as a Gaussian process itself much like the discrepancy in the previous section [21–23]. The choice of a Gaussian process for representing the functional relationship offers the same advantages as in the discrepancy and provides the ability to learn complex input-output relationships at the same computational complexity as simple functions.

The formulation of the model using state-dependent parameters thus becomes

$$y(x) = \eta(x,\theta(x)) + \varepsilon \tag{10}$$

where the calibration parameters, $\theta(x)$ are no longer stationary and are now functions of the same inputs, x, as the experimental data. Following the general approach of Brown and Atamturktur [22] in calibrating models with nonparametric functional parameters the GP functions for each of the calibration parameters can be represented as

$$\theta(x) = \begin{Bmatrix} A(x) \propto GP(\mu_A(x), R_A(x,x')) \\ B(x) \propto GP(\mu_B(x), R_B(x,x')) \\ C(x) \propto GP(\mu_C(x), R_C(x,x')) \\ n(x) \propto GP(\mu_n(x), R_n(x,x')) \\ m(x) \propto GP(\mu_m(x), R_m(x,x')) \end{Bmatrix} \tag{11}$$

where each equation represents the functional representation of each of the Johnson-Cook model parameters, $\mu_i(x)$ represents the mean function for each of the GPs and in this case is treated as a constant with the same prior distribution as in the previous calibration forms, and $R_i(\cdot,\cdot)$ represents the independent covariance function for each functional parameter.

This state-dependent approach will allow the GP for each parameter to uncover, through the same MCMC sampling algorithm, the posterior distribution of the relationship of the input domain to the parameter value. The relationship for each parameter can be used to provide an improved fit between the model output and the data and, in this case, add in the strain, strain rate, and temperature material relationships that may be lacking in the current model form.

State-Dependent Parameters with Discrepancy

The last approach considered in this work is combination of the two previous formulations to add a GP discrepancy term to the state-dependent parameter calibration method. The model form in this case, therefore, becomes

$$y(x) = \eta(x,\theta(x)) + \delta(x) + \varepsilon \tag{12}$$

where both the functional parameter equations and the discrepancy term take the same forms as in Eqn. 7 and Eqn. 11.

In this approach, the Bayesian inference process samples draws from the posteriors of both the state-dependent parameters and the GP discrepancy simultaneously and both of which use the same priors as in the previous approaches.

RESULTS

Based on the data described in the experimental data section, four of the data sets (293K, 0.001/s; 293K, 3250/s; 673K, 0.001/s; 673K, 3600/s) were used to run the each of the calibration approaches. These data sets were chosen to give stress-strain curves across a range of temperatures and strain rates, while retaining some data as holdout to allow for evaluation of the interpolation and extrapolation ability of each approach.

Prior distributions are first established over the model parameters based on a combination of literature review and expert

Downloaded from http://asmedigitalcollection.asme.org/VVS/proceedings-pdf/VVS2020/83594/V001T03A002/6554370/v001t03a002-vvs2020-8816.pdf by Clemson University user on 09 February 2022

knowledge regarding 304L stainless steel. The normal distribution priors for the five parameters are listed in Tab. 2 and are used in each of the four different approaches.

TABLE 2. NORMAL PRIOR DISTRIBUTIONS ON JOHNSON-COOK MODEL PARAMETERS

Parameter	μ	σ
A	160	10
B	1400	50
C	0.017	0.005
n	0.55	0.1
m	0.60	0.1

Using the standard Bayesian calibration approach, posterior distributions for the five Johnson-Cook model parameters are found after carrying out the MCMC algorithm. Figure 2 shows the joint posterior distributions and the mean posterior values for the five parameters. These computed parameter posterior distributions can then be used to make predictions using the model to better understand both the calibrated model output and its associated uncertainty. Though repeated sampling from the posterior distributions, the mean and standard deviation can be computed and then compared to the experimental measurements. Figure 3 shows the posterior mean output values of the calibrated model for each of the four sets of training data. The dotted lines in this figure represent the 95% confidence interval about the mean calibrated output.

Following calibration using the standard Bayesian approach, the Gaussian process discrepancy approach is applied to the problem using the same priors on the parameters and a zero-mean prior on the GP discrepancy function. The results of this approach can be seen compared to the standard Bayesian calibration in Fig. 4 with the standard Bayesian approach in blue and the discrepancy approach in black. Figure 4(a) represents a comparison between the mean model outputs using the calibrated posterior parameter values without the addition of the additive discrepancy. Despite the simultaneous calibration of the parameter values and the additive discrepancy, it can be seen that the resulting model fits to the experimental data are quite similar across the temperature and strain-rate states and Fig. 5 shows the posterior parameter values are quite similar as well.

Alternatively, Fig. 4(b) shows the same mean model outputs, but this time with the discrepancy term added to the second approach. In this case, it can be seen that the discrepancy approach does a much better job of fitting the experimental data and helping to correct for the model bias that is present even after calibration.

The next approach applied is that of the state-dependent parameter calibration. In this approach, the parameters are each

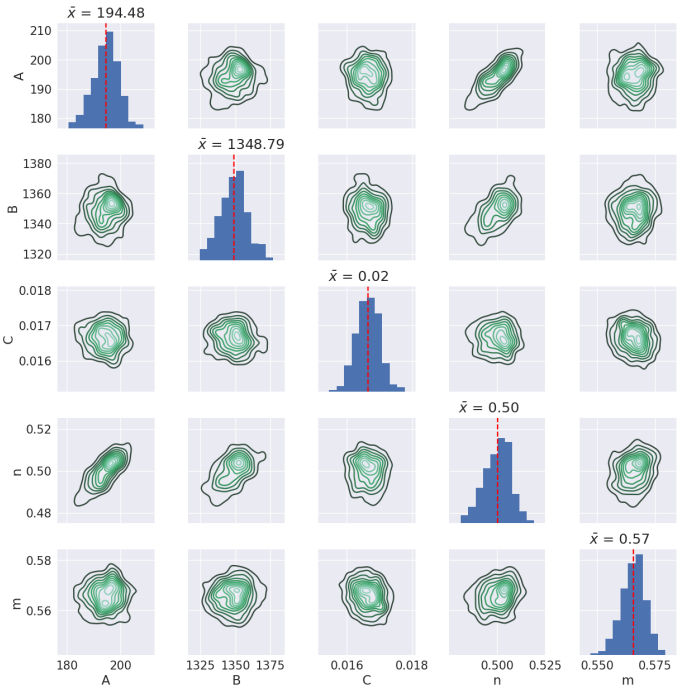

FIGURE 2. JOINT POSTERIOR DISTRIBUTION PLOT FOR THE FIVE JOHNSON-COOK MODEL PARAMETERS COMPUTED USING THE STANDARD BAYESIAN CALIBRATION APPROACH WITHOUT DISCREPANCY

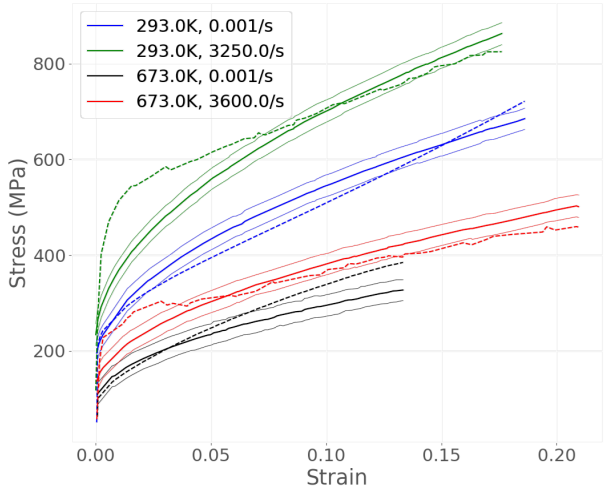

FIGURE 3. MEAN POSTERIOR JOHNSON-COOK MODEL OUTPUT RESULTS COMPARED TO THE EXPERIMENTAL DATA. DOTTED LINES REPRESENT 95% CONFIDENCE INTERVAL ABOUT THE MEAN

treated as a separate GP with a constant, non-zero mean function with a prior distribution equal to those in Tab. 2. Calibration is carried out by exploring the posterior distributions of the parameter functions using MCMC. The result of this process is a GP

Downloaded from http://asmedigitalcollection.asme.org/VVS/proceedings-pdf/VVS2020/83594/V001T03A002/6554370/v001t03a002-vvs2020-8816.pdf by Clemson University user on 09 February 2022

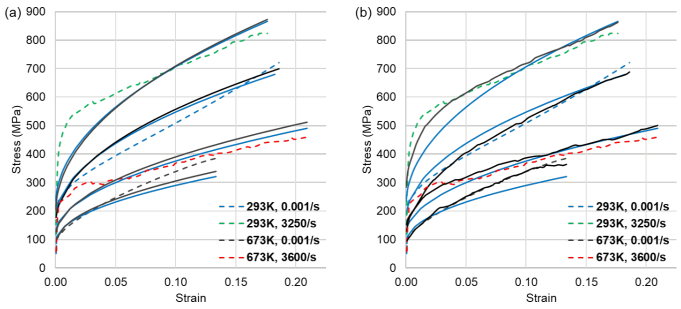

FIGURE 4. COMPARISON BETWEEN THE STANDARD BAYESIAN APPROACH (BLUE) AND THE ADDED DISCREPANCY APPROACH (BLACK). (A) COMPARES THE TWO WITHOUT THE DISCREPANCY ADDED TO THE CALIBRATED OUTPUT AND (B) COMPARES WITH THE ADDITIVE DISCREPANCY

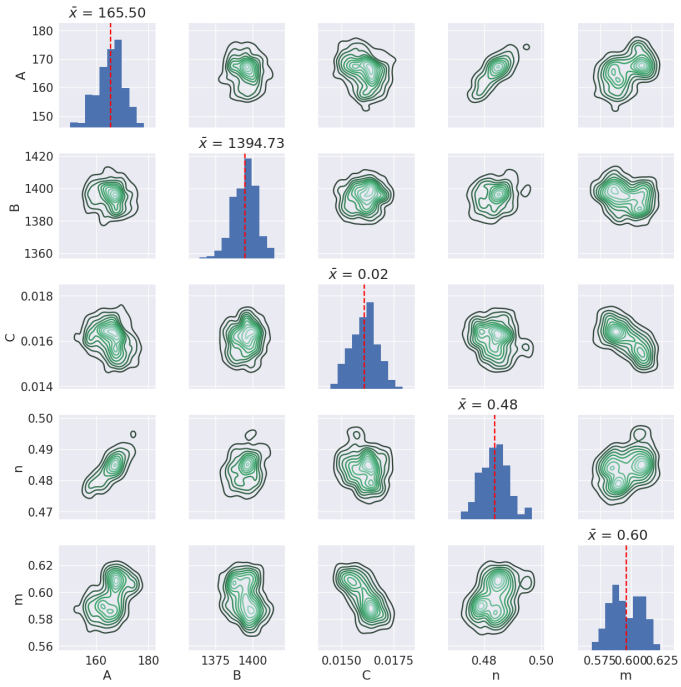

FIGURE 5. JOINT POSTERIOR DISTRIBUTION PLOT FOR THE FIVE JOHNSON-COOK MODEL PARAMETERS COMPUTED USING THE BAYESIAN CALIBRATION APPROACH WITH DISCREPANCY

for each parameter that can be evaluated to obtain a parameter distribution at each value of strain, strain-rate, and temperature.

This calibration is then carried out again for the state-dependent approach with an additive GP discrepancy term. The results of all four calibration approaches are shown Tab. 3. The table compares the RMS error for each of the four calibration methods (standard Bayesian, discrepancy, state-dependent, and state-dependent with discrepancy) when the mean calibrated model output is compared to the four calibration data sets. In general, as each of the approaches increase in complexity, the overall error improves compared to the previous approach.

TABLE 3. COMPARISON OF THE COMPUTED RMS ERROR FOR THE CALIBRATION APPROACHES

Data set	Method 1	Method 2	Method 3	Method 4
293K, 0.001/s	49.9	32.2	34.5	29.3
293K, 3250/s	61.0	35.3	20.1	16.0
673K, 0.001/s	37.3	8.4	8.2	14.0
673K, 3600/s	28.4	24.8	15.9	17.8

Figure 6 illustrates the comparison between the discrepancy approach and the state-dependence with discrepancy approach when looking at the respective values of the strain-hardening exponent, n, in the Johnson-Cook model and the mean posterior values of the discrepancy function. The discrepancy approach in Fig. 6(a) illustrates the stationary value for n across the strain, temperature, and strain-rate domain and the value of the GP discrepancy can be seen to vary across the input domain to account for the bias present in the material model, despite parameter calibration. Alternatively, in the state-dependent approach, shown in Fig. 6(b), n varies across the input domain, while the value for the GP discrepancy becomes essentially superflous and remains at its prior value of zero even after calibration. This indicates that the bias present in the model is being taken up by the calibrated, functional parameter relationships instead of the additive discrepancy term.

While observing the value of the model discrepancy function can help the model creator locate and reduce model bias, the experimentally-informed parameter relationships can provide a more interpretable understanding of bias in specific components of the model form. For example, the slope of the value of n increases as a function of strain at higher strain-rates and the y-intercept of the function increases with temperature, but only at high strain-rates. At low strain-rates, the value of n is relatively constant across temperature and strain. This relationship indicates a model bias in the treatment of the strain-hardening exponent that does not properly account for the complete temperature and strain-rate dependence present in the experimental data. A better understanding of this relationship can, therefore, provide a directed path for model improvement compared to measures of the overall model bias, like the discrepancy term.

Prediction Validation

In order to rely on the results of any model calibration approach, it is important to be able to understand and quantify the uncertainty about model output when using the model in areas

Downloaded from http://asmedigitalcollection.asme.org/VVS/proceedings-pdf/VVS2020/83594/V001T03A002/6554370/v001t03a002-vvs2020-8816.pdf by Clemson University user on 09 February 2022

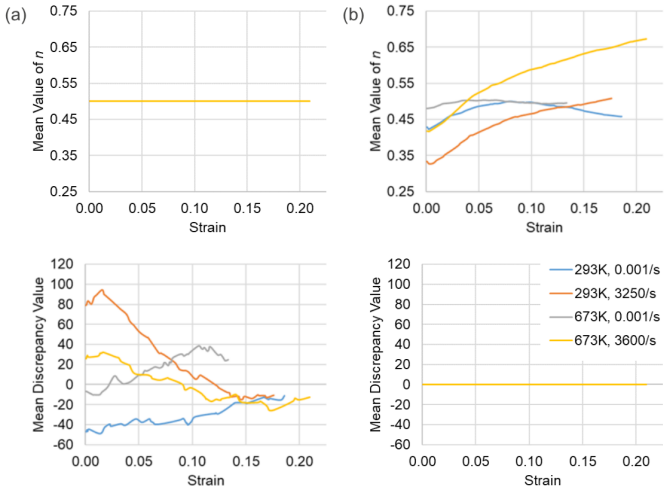

FIGURE 6. PLOT OF THE MEAN VALUE OF THE *N* PARAMETER AND THE DISCREPANCY VALUE FOR THE (A) STATIONARY APPROACH WITH DISCREPANCY AND THE (B) STATE-DEPENDENT APPROACH WITH DISCREPANCY

of the input domain that were not used for calibration. This becomes especially important in many material models, when real-world conditions are beyond that which can be tested and measured accurately in a laboratory setting. In this work, two sets of data from the experimental campaign were selectively chosen as holdout to compare the described calibration approaches in their relative accuracy when tested over new data. The two data sets are 293K, 0.1/s and 873K, 3500/s, which are at input values within the calibration domain and beyond the calibration domain, respectively. Therefore, the first set serves as a validation set for the calibration approaches and the second serves to assess the extrapolation ability of the approaches.

Figure 7 shows the comparison between the standard Bayesian, discrepancy, and stat-dependent approaches when validated against the holdout data sets. As can be seen in Fig. 7(a), at a new temperature and strain-rate within the calibration domain, all three approaches provide results that are very similar in accuracy to the true experimental data (with the state-dependent model providing a better capture of the linear stress-strain relationship that the other two). This is to be expected with a well-calibrated model and is a positive indication as to the reliability of the models when serving as a predictor for material behavior.

In Fig. 7(b), however, it can be seen that the state-dependent calibration performs better than either of the other two approaches when extrapolating into a new temperature domain. This is due to the fact that outside of the calibration input domain, the value of the discrepancy GP returns to the mean zero prior value due to the lack of experimental data. The state-dependent model, on the other hand, can continue to extrapolate the learned parameter relationships for each of the parameters according to the posterior mean value of each GP with smoother functions

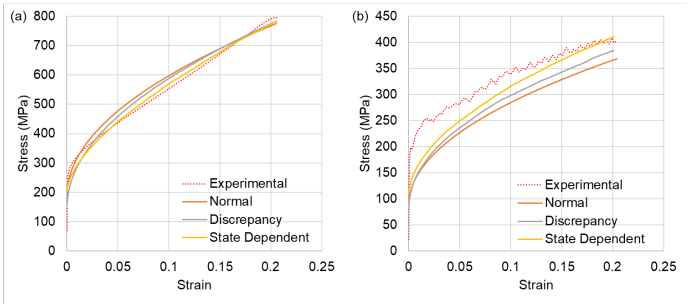

FIGURE 7. MEAN MODEL OUTPUT RESULTS FOR THE TWO VALIDATION DATA SETS: 293K, 0.1/S (A) AND 873K, 3500/S (B)

that are essentially filtered through the model itself (see Fig. 6). Thus, the state-dependent model calibration that provides generally improved RMS errors compared to discrepancy calculation can have greater extrapolation accuracy than the other approaches.

CONCLUSIONS

With the goal of accurately predicting the performance of materials under dynamic loading conditions, models have been developed that describe the rate-dependent material behavior and irrecoverable plastic deformation that occurs at elevated strains and applied loads. These models generally require the addition of specific parameters for individual materials and systems. In this work, we presented a systematic approach to the problem of calibrating a Johnson-Cook plasticity model for 304L stainless steel in which the parameters are treated as dependent on the state of the material and uncovered using experimental data.

The use of state-dependent Bayesian parameter calibration in determining values of the parameters of the Johnson-Cook model for 304L stainless steel has the demonstrated the ability to produce better model agreement with the experimental data used for calibration compared to the other calibration approaches described in this work. The results obtained during the model calibration indicate that the proposed approach of defining parameters using state-dependent, nonparametric functions based on Gaussian processes can make the presence of an additive discrepancy term in the calibration formulation unnecessary and, at the same time, improve the extrapolation prediction accuracy of the model into new input domains. Additionally, the results of the calibrated functional relationships of the parameters can be examined to provide an experimentally-informed and more interpretable assessment of the Johnson-Cook model form bias that exists over the input domain compared to additive discrepancy terms that can only describe to overall model bias. This improved interpretability of the physics-based bias serves as a direct method to extend the model formulation to improve the model fit for new materials and input domains.

The improved parameter dependence understanding gained through this work has served to improve the Johnson-Cook pre-

Downloaded from http://asmedigitalcollection.asme.org/VVS/proceedings-pdf/VVS2020/83594/V001T03A002/6554370/v001t03a002-vvs2020-8816.pdf by Clemson University user on 09 February 2022

dictive accuracy for 304L stainless steel and has led to methods to extend the original model definition to account for the discrovered model bias. Further work should be carried out to apply the state-dependent Bayesian calibration to more materials using the Johnson-Cook model and to further material models.

ACKNOWLEDGMENT

Thanks go to Shuh-Rong Chen of the MST-8 group at Los Alamos National Laboratory for collecting and providing the experimental data used in this work.

REFERENCES

[1] Perzyna, P., 1966. "Fundamental problems in viscoplasticity". *Advances in Applied Mechanics,* ***9***, pp. 243–377.

[2] Follansbee, P. S., and Kocks, U. F., 1988. "A constitutive description of the deformation of copper based on the use of the mechanical threshold stress as an internal state variable". *Acta Metallurgica,* ***36***(1), pp. 81–93.

[3] Kocks, U. F., 2001. "Realistic constitutive relations for metal plasticity". *Materials Science and Engineering: A,* ***317***, pp. 181–187.

[4] Zerilli, F. J., and Armstrong, R. W., 1987. "Dislocation-mechanics-based constitutive realtions for material dynamics calculations". *Journal of Applied Physics,* ***61***(5), pp. 1816–1825.

[5] Preston, D. L., Tonks, D. L., and Wallace, D. C., 2003. "Model of plastic deformation for extreme loading conditions". *Journal of Applied Physics,* ***93***(1), pp. 211–220.

[6] Johnson, G. R., and Cook, W. H., 1985. "Fracture characteristics of three metals subjected to various strains, strain rates, temperatures, and pressures". *Engineering Fracture Mechanics,* ***21***(1), pp. 31–48.

[7] Steinberg, D. J., Cochran, S. G., and Guinan, M. W., 1980. "A constitutive model for metals applicable at high-strain rate". *Journal of Applied Physics,* ***51***(3), pp. 1498–1504.

[8] Steinberg, D. J., and Lund, C. M., 1989. "A constitutive model for strain rates from 10^{-4} to 10^{6} s^{-1}". *Journal of Applied Physics,* ***65***(4), pp. 1528–1533.

[9] Gambirasio, L., and Rizzi, E., 2014. "On the calibration strategies of the Johnson–Cook strength model: Discussion and applications to experimental data". *Materials Science and Engineering: A,* ***610***, pp. 370–413.

[10] Shin, H., and Kim, J.-B., 2019. "Evolution of specimen strain rate in split Hopkinson bar test". *Proceedings of the Institution of Mechanical Engineers,* ***233***(13), pp. 4667–4687.

[11] Sarva, S., Mulliken, A. D., and Boyce, M. C., 2007. "Mechanics of Taylor impact testing of polycarbonate". *International Journal of Solids and Structures,* ***44***, pp. 2381–2400.

[12] Kennedy, M. C., and O'Hagan, A., 2001. "Bayesian calibration of computer models". *J. R. Statist. Soc,* ***63***, pp. 425–464.

[13] Higdon, D., Gattiker, J., Williams, B., and Rightley, M., 2008. "Computer model calibration using high-dimensional output". *Journal of the American Statistical Association,* ***103***(482), pp. 570–583.

[14] Williams, B., Higdon, D., Gattiker, J., Moore, L., McKay, M., and Keller-McNulty, S., 2006. "Combining experimental data and computer simulations, with an application to flyer plate experiments". *Baysn Anal.,* ***1***, pp. 765–792.

[15] Bayarri, M. J., Berger, J. O., Cafeo, J., Garcia-Donato, G., Liu, F., Palomo, J., Parthasarathy, R. J., Paulo, R., Sacks, J., and Walsh, D., 2007. "Computer model validation with functional output". *Ann,* ***35***, pp. 1874–1906.

[16] Geman, S., and Geman, D., 1984. "Stochastic relaxation, gibbs distributions and the Bayesian restoration of images". *IEEE Transactions on Pattern Analysis and Machine Intelligence,* ***6***, pp. 721–741.

[17] Tierney, L., 1994. "Markov chains for exploring posterior distributions". *Annals of Statistics,* ***22***, pp. 1701–1762.

[18] Rasmussen, C. E., and Williams, C., 2006. *Gaussian Processes for Machine Learning, Cambridge: MIT Press*.

[19] Fugate, M., Williams, B., Higdon, D., Hanson, K. M., Gattiker, J., Chen, S.-R., and Unal, C., 2006. Hierarchical Bayesian analysis and the Preston-Tonks-Wallace model. Tech. rep., Los Alamos National Laboratory Technical Report: LA-UR-06-5205.

[20] Atamturktur, S., Hegenderfer, J., Williams, B., Egeberg, M., Lebensohn, R. A., and Unal, C., 2015. "A resource allocation framework for experimental-based validation of numerical models". *Mechanics of Advanced Materials and Structures,* ***22***, pp. 641–654.

[21] Plumlee, M., Joseph, V. R., and Yang, H., 2016. "Calibrating functional parameters in the ion channel models of cardiac cells". *Journal of the American Statistical Association,* ***111***(514), pp. 500–509.

[22] Brown, D. A., and Atamturktur, S., 2018. "Nonparametric functional calibration of computer models". *Statistica Sinica,* ***28***, pp. 721–742.

[23] Atamturktur, S., and Brown, D. A., 2015. "State-aware calibration for inferring systemic bias in computer models of complex systems". In *NAFEMS World Conference Proceedings, June 21-24, San Diego, CA*.

Downloaded from http://asmedigitalcollection.asme.org/VVS/proceedings-pdf/VVS2020/83594/V001T03A002/6554370/v001t03a002-vvs2020-8816.pdf by Clemson University user on 09 February 2022